Inorg. Chem. **2007**, *46*, 7621–7632

Diphenyl(dipyrazolyl)methane Complexes of Ni: Synthesis, Structural Characterization, and Chromotropism of $NiBr_2$ Derivatives

Natalie Baho and Davit Zargarian*

Département de Chimie, Université de Montréal, C. P. 6128, Succursale Centre-ville, Montréal, Québec, Canada H3C 3J7

Received January 18, 2007

The reaction of $NiBr_2$ with the bidentate ligand diphenyl(dipyrazolyl)methane (dpdpm) gives the pentacoordinated complexes [(dpdpm)Ni(μ-Br)Br]$_2$ (**1**), [(dpdpm)$NiBr_2(H_2O)$] (**2a**), and [(dpdpm)$NiBr(H_2O)_2$]Br (**2b**), or the octahedral complexes [(dpdpm)$NiBr(H_2O)_2(CH_3CN)$]Br (**3**), [(dpdpm)$_2NiBr_2$] (**4**), and [(dpdpm)$_2NiBr(H_2O)$]Br (**5**). All of these complexes are paramagnetic, both in the solid state and in solution, and have been characterized by spectroscopic (IR, NMR, and UV–vis–NIR) and X-ray diffraction studies. The unoccupied coordination site in the pentacoordinated compounds allows long-range interactions, in the solid state, between the Ni center and a Ph substituent of the dpdpm ligand. These weak interactions are replaced by Ni–solvent interactions, both in the solid state and in solution, facilitating the interconversion of these compounds under various reaction conditions and leading to interesting solvato-, vapo-, and thermochromic properties. UV–vis–NIR spectroscopy has been used to study these phenomena. Absorption spectra for the room-temperature methanol or acetonitrile solutions of the pentacoordinate or octahedral compounds show three main bands in the region of 350–1000 nm that represent spin-allowed (d–d) transitions from the ground state $^3A_{2g}$ to the excited states $^3T_{2g}$, $^3T_{1g}(^3F)$, and $^3T_{1g}(^3P)$. A weak shoulder was also detected on the middle peak in most spectra (700–800 nm), representing the spin-forbidden $^3A_{2g} \rightarrow {}^1Eg$ transition. On the other hand, the spectra of high-temperature CH_2Cl_2 or acetone solutions of all complexes show four main bands at ca. 490, 650–660, 860, and 1000 nm, in addition to a shoulder on the first or second band.

Introduction

Scorpionate-type poly(pyrazolyl)borate[1] and poly(pyrazolyl)alkane[2] ligands have found wide applications in coordination, organometallic, and bioinorganic chemistry.[3] The increasing interest in these ligands is due to their generally robust nature and the ease with which their steric and electronic properties can be modified via simple synthetic protocols, thereby allowing a fine-tuning of ligand properties.[4] The anionic bis- or tris(pyrazolyl)borates have been used in the preparation of a wide range of coordination and organometallic complexes, including species featuring metals

* To whom correspondence should be addressed. Tel: 514-343-2247. Fax: 514-343-2468. E-mail: zargarian.davit@umontreal.ca.

(1) (a) Trofimenko, S.; Calabrese, J. C.; Thompson, S. J. *Inorg. Chem.* **1987**, *26*, 1507. (b) Trofimenko, S. *J. A. Chem. Soc.* **1970**, *92*, 5118. (c) Trofimenko, S.; Calabrese, J. C.; Domaille, P. J.; Thompson, J. S. *Inorg. Chem.* **1989**, *28*, 1091. (d) Paulo, A.; Correia, J. D. G.; Santos, I. *Rev. Inorg. Chem.* **1998**, *5*, 57. (e) Uehara, K.; Hikichi, S.; Akita, M. *J. Chem. Soc., Dalton Trans.* **2002**, 3529. (f) Santi, R.; Romano, A. M.; Sommazzi, A.; Grande, M.; Bianchini, C.; Mantovani, G. *J. Mol. Catal. A: Chem.* **2005**, *229*, 191. (g) Shirasawa, N.; Nguyet, T.-T.; Hikichi, S.; Moro-oka, Y.; Akita, M. *Organometallics* **2001**, *20*, 3582. (h) Kisala, J.; Ciunik, Z.; Drabent, K.; Ruman, T.; Wolowiec, S. *Polyhedron* **2003**, *22*, 1645. (i) Rheingold, A. L.; Haggerty, B. S.; Liable-Sands, L. M.; Trofimenko, S. *Inorg. Chem.* **1999**, *38*, 6306. (j) Malbosc, F.; Chauby, V.; Serra-Le Berre, C.; Etienne, M.; Daran, J.; Kalck, P. *Eur. J. Inorg. Chem.* **2001**, 2689.

(2) Trofimenko, S. *J. Am. Chem. Soc.* **1970**, *92*, 1499.

(3) For a few recent reports and reviews on the development of the coordination chemistry of scorpionate ligands see: (a) Tang, T.; Wang, Z.; Xu, Y.; Wang, J.; Wang, H.; Yao, X. *Polyhedron* **1999**, *18*, 2383. (b) Sánchez, G.; Serrano, L. J.; Pérez, J.; Ramírez de Arellano, M. C.; López, G.; Molins, E. *Inorg. Chim. Acta* **1999**, *295*, 136. (c) Seymore, S. B.; Brown, S. N. *Inorg. Chem.* **2000**, *39*, 325. (d) Tang, L.-F.; Wang, Z.; Jia, W.-L.; Xu, Y.-M.; Wang, J.-T. *Polyhedron* **2002**, *19*, 381. (e) Burzlaff, N.; Hegelmann, I.; Weibert, B. *J. Organomet. Chem.* **2001**, *626*, 16. (f) Mattini, D.; Pellei, M.; Pettinari, C.; Skelton, B. W.; White, A. H. *Inorg. Chim. Acta* **2002**, *333*, 72. (g) Wang, Z.-H.; Tang, L.-F.; Jia, W.-L.; Wang, J.-T.; Wang, H.-G. *Polyhedron* **2002**, *21*, 873. (h) Kläui, W.; Berghahn, M.; Frank, W.; Reiss, G. J.; Schönherr, T.; Rheinwald, G.; Lang, H. *Eur. J. Inorg. Chem.* **2003**, 2059. (i) Mahon, M. F.; McGinley, J.; Molloy, K. C. *Inorg. Chim. Acta* **2003**, *355*, 368. (j) Otero, A.; Fernandez-Baeza. J.; Antinolo, A.; Tejeda, J.; Lara-Sánchez, A. *Dalton Trans.* **2004**, 1499. (k) Pettinari, C.; Pettinari, R. *Coord. Chem. Rev.* **2005**, *249*, 663. (l) Tredget, C. S.; Lawrence, S. C.; Ward. B. D.; Howe, R. G.; Cowley, A. R.; Mountford, P. *Organometallics* **2005**, *24*, 3136. (m) Montoya, V.; Pons, J.; Solans, X.; Font-bardia, M.; Ros, J. *Inorg. Chim. Acta* **2005**, *358*, 2312. (n) Pettinari, C.; Pettinari, R. *Coord. Chem. Rev.* **2005**, *249*, 525.

10.1021/ic070093m CCC: $37.00
Published on Web 08/01/2007

in their less common oxidation states such as Pd(IV)[5,6] and Pt(IV).[5,7] In contrast, the neutral bis- and tris(pyrazolyl)-alkanes appear to be less suitable for the preparation of complexes featuring strong-field co-ligands such as hydride, alkyls, aryls, etc.[8] As a result, poly(pyrazolyl)alkanes have had less impact in organometallic chemistry, particularly in the case of late transition metals of the first row such as nickel for which no organometallic complex has been reported.[9,10]

Our interest in the chemistry of organonickel complexes[11] has prompted us to explore the structures and reactivities of nickel complexes based on poly(pyrazolyl)alkanes. Our initial studies focused on the reactions of $Ni(NO_3)_2$ with the ligands bis- and tris(3,5-dimethylpyrazolyl)methane (bpm* and tpm*),[12] bis(pyrazolyl)propane (bpp),[13] and diphenyl(dipyrazolyl)methane (dpdpm).[14] The complexes arising from these reactions are octahedral species featuring mono- and/or bidentate nitrate ligands. Our results to date show that these compounds cannot serve as suitable precursors for the preparation of organometallic species, but many of them exhibit interesting solvato-, vapo-, and thermochromic properties, owing to the labile coordination of the nitrate ligand.[14] Indeed, literature reports show that several nickel complexes featuring polydentate amine or imine-type ligands display solvato- and thermochromic behavior arising from displacement of labile ligands by solvent molecules or counterions. In the case of coordination complexes, solvatochromism refers to changes in the electronic absorption spectra due to weak dipole interactions or hydrogen bonds with solvent molecules or a strong and specific interaction between the solvent and the metal center.[15] Solvato- and thermochromism can also involve various types of structural isomerism such as monomer−dimer equilibria, some examples of which have been reported for $[Ni(L-L)Cl_2]_2$ wherein L−L is a bidentate, N-based ligand.[16]

As a continuation of our earlier studies,[12−14] we are investigating the structures and chromotropic properties of complexes arising from the reactions of other nickel(II) salts with poly(pyrazolyl)alkane ligands. The present report describes the synthesis, structural characterization, and solvato-, vapo-, and thermochromic behavior of the $NiBr_2$ derivatives of dpdpm, namely, $[(dpdpm)Ni(\mu\text{-}Br)Br]_2$ (**1**), $[(dpdpm)NiBr_2(H_2O)]$ (**2a**), $[(dpdpm)NiBr(H_2O)_2]Br$ (**2b**), $[(dpdpm)NiBr(H_2O)_2(CH_3CN)]Br$ (**3**), $[(dpdpm)_2NiBr_2]$ (**4**), and $[(dpdpm)_2NiBr(H_2O)]Br$ (**5**). Complexes featuring the dpdpm ligand have been reported for Cu,[17] Mo,[18] Ag,[19] and Pd.[10c]

Results and Discussion

Synthesis of the Complexes. The outcome of the reaction between $NiBr_2$ and dpdpm depends on a few parameters,

(4) Byers, P. K.; Canty, A. J.; Honeyman, R. T. *Adv. Organomet. Chem.* **1992**, *34*, 1. (See in particular pp 26 and 34.)

(5) Canty, A. J.; Andrew, S.; Skelton, B. W.; Traill, P. R.; White, A. H. *Organometallics* **1995**, *14*, 199.

(6) (a) Hill, M. S.; Mahon, M. F.; Mcginley, J. M. G.; Molloy, K. C. *Polyhedron* **2001**, *20*, 1995. (b) Reger, D. L.; Grattan, T. C.; Brown, K. J.; Little, C. A.; Lamba, J. J. S.; Rheingold, A. L.; Sommer, R. D. *J. Organomet. Chem.* **2000**, *607*, 120.

(7) Reinartz, S.; Brookhart, M.; Templeton, J. L. *Organometallics* **2002**, *21*, 247.

(8) Byers, P. K.; Canty, A. J.; Skelton, B. W.; White, A. H. *Organometallics* **1990**, *9*, 826.

(9) For representative reports on coordination complexes of Ni featuring poly(pyrazolyl)alkane ligands see: (a) Mahon, M. F.; McGinley, J.; Molloy, K. C. *Inorg. Chim. Acta* **2003**, *355*, 368. (b) Wolfgang, K.; Berghahn, M.; Frank, W.; Reiss, G. J.; Schonherr, T.; Rheinwald, G.; Lang, H. *Eur. J. Inorg. Chem.* **2003**, *11*, 2059. (c) Pettinari, C.; Marchetti, F.; Cingolani, A.; Leonesi, D.; Colapietro, M.; Margadonna, S. *Polyhedron* **1998**, *17*, 4145. (d) Mann, K. L.; Jeffery, J. C.; McCleverty, J. A.; Thornton, P.; Ward, M. D. *J. Chem. Soc., Dalton Trans.* **1998**, *1*, 89. (e) Pettinari, C.; Cingolani, A.; Bovio, B. *Polyhedron* **1996**, *15*, 115. (f) Astley, T.; Gulbis, J. M.; Hitchman M. A.; Tiekink, E. R. T. *J. Chem. Soc., Dalton Trans.* **1993**, 509. (g) Mesubi, M. A.; Omotowa, B. A. *Synth. React. Inorg. Metal-Org. Chem.* **1993**, *23*, 213. (h) Astley, T.; Canty, A. J.; Hitchman, M. A.; Rowbottom, G. L.; Skelton, B. W.; White, A. H. *J. Chem. Soc., Dalton Trans.* **1991**, 1981. (i) Reedijk, J.; Verbiest, J. *Trans. Met. Chem.* **1979**, *4*, 239. (j) Jansen, J. C.; Van Koningsveld, H.; Van Ooijen, J. A. C.; Reedijk, J. *Inorg. Chem.* **1980**, *19*, 170. (k) Reedijk, J.; Verbiest, J. *Trans. Met. Chem.* **1978**, *3*, 51.

(10) For recent reports on organometallic complexes of Pd based on poly-(pyrazolyl)alkane ligands see: (a) Sanchez, G.; Serrano, L. J.; Pérez, J.; Ramirez de Arellano, M. C.; Lopez, G.; Molins, E. *Inorg. Chim. Acta* **1999**, *295*, 136. (b) Arroyo, N.; Gomez-de La Tore, F.; Jalon, A. F.; Manzano, B. R.; Moreno-Lara, B.; Rodriguez, A. M. *J. Organomet. Chem.* **2000**, *603*, 174. (c) Tsuji, S.; Swenson, D. C.; Jordan, R. F. *Organometallics* **1999**, *18*, 4758.

(11) (a) Castonguay, A.; Sui-Seng, C.; Zargarian, D.; Beauchamp, A. L. *Organometallics* **2006**, *25*, 602. (b) Groux, L. F.; Bélanger-Garlépy, F.; Zargarian, D. *Can. J. Chem.* **2005**, *83*, 634. (c) Gareau, D.; Sui-Seng, C.; Groux, L. F.; Brisse, F.; Zargarian, D. *Organometallics* **2005**, *24*, 4003. (d) Chen, Y.; Sui-Seng, C.; Zargarian, D. *Angew. Chem., Int. Ed.* **2005**, *44*, 7721. (e) Boucher, S.; Zargarian, D. *Can. J. Chem.* **2005**, *84*, 233. (f) Chen, Y.; Sui-Seng, C.; Boucher, S.; Zargarian, D. *Organometallics* **2005**, *24*, 149. (g) Fontaine, F.-G.; Zargarian, D. *J. Am. Chem. Soc.* **2004**, *126*, 8786. (h) Groux, L. F.; Zargarian, D. *Organometallics* **2003**, *22*, 4759. (i) Fontaine, F.-G.; Nguyen, R.-V.; Zargarian, D. *Can. J. Chem.* **2003**, *81*, 1299. (j) Groux, L. F.; Zargarian, D. *Organometallics* **2003**, *22*, 3124. (k) Groux, L. F.; Zargarian, D.; Simon, L. C.; Soares, J. B. P. *J. Mol. Catal. A* **2003**, *19*, 51. (l) Rivera, E.; Wang, R.; Zhu, X. X.; Zargarian, D.; Giasson, R. *J. Molec. Catal. A* **2003**, *204−205*, 325. (m) Zargarian, D. *Coord. Chem. Rev.* **2002**, *233−234*, 157. (n) Wang, R.; Groux, L. F.; Zargarian, D. *Organometallics* **2002**, *21*, 5531. (o) Wang, R.; Groux, L. F.; Zargarian, D. *J. Organomet. Chem.* **2002**, *660*, 98. (p) Fontaine, F.-G.; Zargarian, D. *Organometallics* **2002**, *21*, 401. (q) Dubois, M.-A.; Wang, R.; Zargarian, D.; Tian, J.; Vollmerhaus, R.; Li, Z.; Collins, S. *Organometallics* **2001**, *20*, 663. (r) Groux, L. F.; Zargarian, D. *Organometallics* **2001**, *20*, 3811. (s) Groux, L. F.; Zargarian, D. *Organometallics* **2001**, *20*, 3811. (t) Fontaine, F.-G.; Dubois, M.-A.; Zargarian, D. *Organometallics* **2001**, *20*, 5156. (u) Wang, R.; Bélanger-Gariépy, F.; Zargarian, D. *Organometallics* **1999**, *18*, 5548. (v) Fontaine, F.-G.; Kadkhodazadeh, T.; Zargarian, D. *Chem. Commun.* **1998**, 1253. (w) Vollmerhaus, R.; Bélanger-Gariépy, F.; Zargarian, D. *Organometallics* **1997**, *16*, 4762. (x) Huber, T. A.; Bayrakdarian, M.; Dion, S.; Dubuc, I.; Bélanger-Gariépy, F.; Zargarian, D. *Organometallics* **1997**, *16*, 5811. (y) Bayrakdarian, M.; Davis, M. J.; Reber, C.; Zargarian, D. *Can. J. Chem.* **1996**, *74*, 2194. (z) Huber, T. A.; Bélanger-Gariépy, F.; Zargarian, D. *Organometallics* **1995**, *14*, 4997.

(12) (a) Michaud, A.; Fontaine, F.-G.; Zargarian, D. *Inorg. Chim. Acta.* **2006**, *359*, 2592. (b) Nolet, M.-C.; Michaud, A.; Bain, C.; Zargarian, D.; Reber, C. *Photochem. Photobiol.* **2006**, *82*, 57. (c) Michaud, A.; Fontaine, F.-G.; Zargarian, D. *Acta Crystallogr.* **2005**, *E61*, m784. (b) Michaud, A.; Fontaine, F.-G.; Zargarian, D. *Acta Crystallogr.* **2005**, *E61*, m904.

(13) Michaud, A. M. Sc. Desertation, Université de Montréal, 2004.

(14) Baho, N.; Zargarian, D. *Inorg. Chem.* **2007**, *46*, 299.

(15) For a detailed discussion of these and similar phenomena see: (a) Morassi, R.; Bertini, I.; Sacconi, L. *Coord. Chem. Rev.* **1973**, *11*, 343. (b) Reichardt, C. *Angew. Chem., Int. Ed. Engl.* **1965**, *4*, 29.

(16) (a) Bloomquist, D. R.; Willett, R. D. *Coord. Chem. Rev.* **1982**, *47*, 125. (b) Fabbrizzi, L.; Micheloni, M.; Paoletti, P. *Inorg. Chem.* **1974**, *13*, 1974.

(17) Shaw, J. L.; Cardon, T. B.; Lorigan, G. A.; Ziegler, C. J. *Eur. J. Inorg. Chem.* **2004**, *1073*.

(18) Shiu, K.-B.; Yeh, L.-Y.; Peng. S.-M.; Cheng, M.-C. *J. Organomet. Chem.* **1993**, *460*, 203.

(19) Reger, L. D.; Gardinier, J. R.; Smith, M. D. *Inorg. Chem.* **2004**, *43*, 3825.

Scheme 1

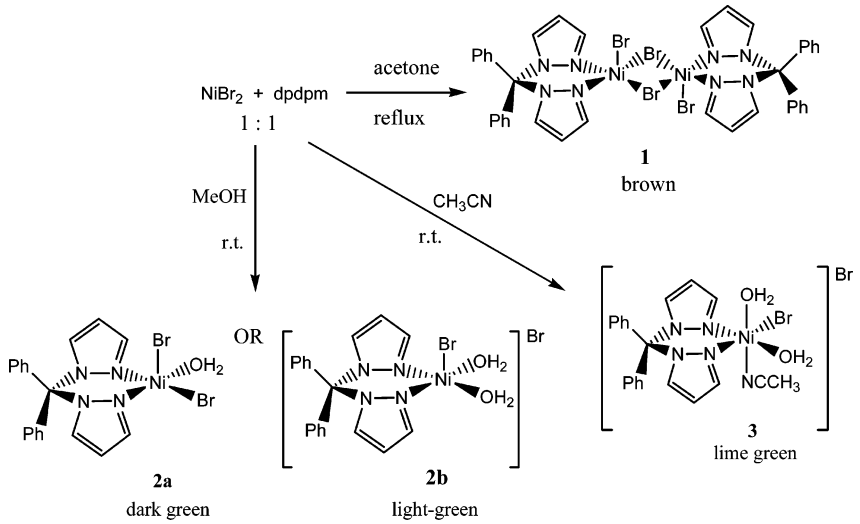

Scheme 2

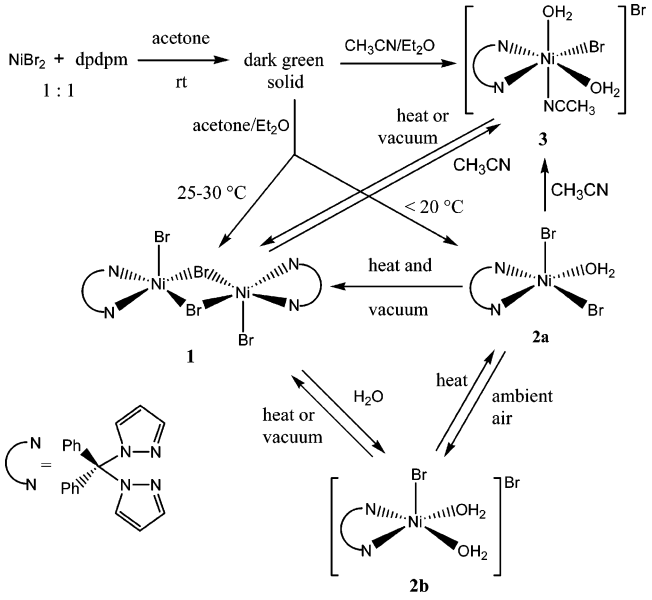

including the metal/ligand ratio, the reaction temperature, the coordinating ability of the solvent, and the degree of residual moisture present in the reaction medium. Thus, refluxing a 1:1 mixture of $NiBr_2$ and dpdpm in dried and distilled acetone for 18 h gave a brown suspension, which was filtered to give a brown solid identified as the dimeric species **1** (crude yield 79%, Scheme 1). In contrast, carrying out the reaction in untreated MeOH at room temperature gave a dark green solid (crude yield 83%) that provided, after recrystallization from acetone/Et_2O, dark green crystals identified as the monomeric, mono(aquo) compound **2a**. Interestingly, recrystallizing the dark green solid from acetone/hexane gave light green crystals identified as the cationic bis(aquo) species **2b**. Finally, overnight stirring of a 1:1 mixture of $NiBr_2$ and dpdpm in acetonitrile at room temperature gave a dark green solution; removal of the solvent produced a dark green powder (crude yield 85%), which was recrystallized from acetonitrile/Et_2O to give lime green crystals of the octahedral species **3**.

It is noteworthy that, under appropriate recrystallization conditions, all of the new products mentioned above can be derived from a common species obtained from the 1:1 reaction of $NiBr_2$ and dpdpm in acetone at room temperature, as shown in Scheme 2. Thus, allowing Et_2O vapors to diffuse into concentrated acetone solutions of the dark green solid at 25−30 °C and with minimum exposure to humid air gave brown crystals that were identified by X-ray diffraction studies as **1**. Alternatively, recrystallization from acetone/Et_2O solutions at lower temperatures (<20 °C) resulted in the formation of dark green crystals that were identified by X-ray diffraction studies as the mono(aquo) compound **2a**. Recrystallization attempts at around 0 °C gave blue crystals, presumably an octahedral bis(aquo) adduct, but we were unable to characterize this compound because of the poor quality of the crystals obtained. Finally, recrystallization of the dark green solid from acetonitrile gave lime green crystals that were identified as **3**.

These mono(dpdpm) derivatives can also interconvert under various experimental conditions (Scheme 2). For instance, allowing brown crystals of **1** to stand overnight in the (green) mother liquor, unprotected from ambient atmosphere, turned them into light green crystals that were

Scheme 3

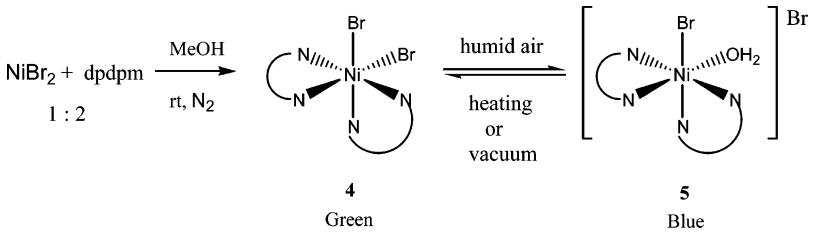

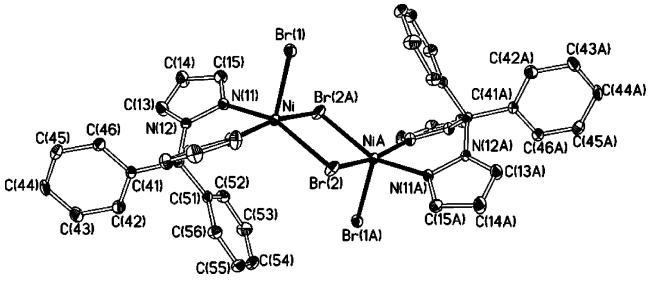

Figure 1. ORTEP view of complex **1**. Thermal ellipsoids are shown at 30% probability.

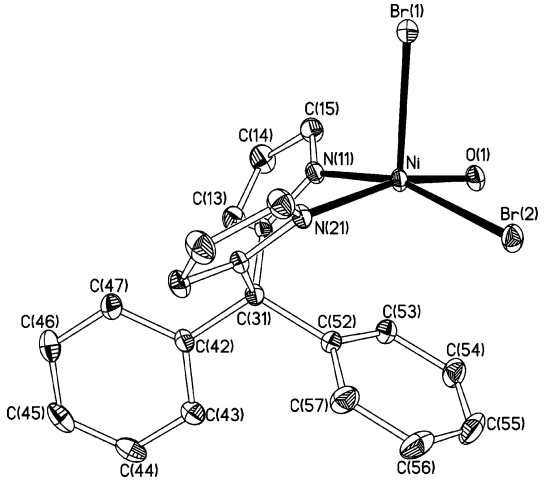

Figure 2. ORTEP view of complex **2a**. Thermal ellipsoids are shown at 30% probability.

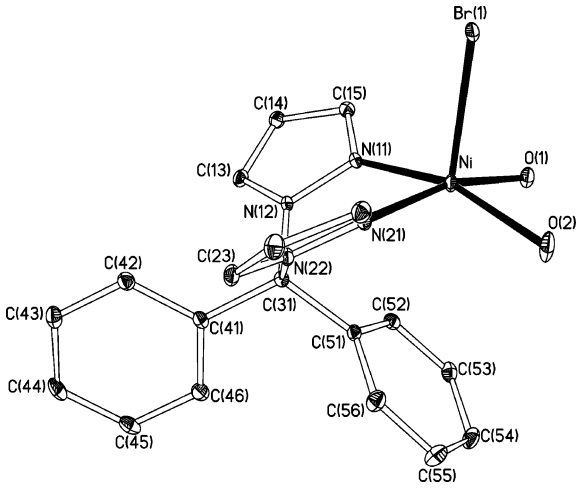

Figure 3. ORTEP view of complex **2b**. Thermal ellipsoids are shown at 30% probability. The Br^- counterion has been omitted for clarity.

identified as **2b**. The latter compound was also obtained by allowing the mono(aquo) species **2a** to stand in ambient atmosphere for 2 days or more, while dissolving **2a** in CH_3CN gave the octahedral species **3**. On the other hand, heating solid samples of **2b** or **3** to ca. 100 °C or placing them under reduced pressure converts these compounds to **1**. In the case of **2a**, both heating and reduced pressure were needed to convert this compound to **1**. As will be mentioned later, the interconversion of complexes **1**, **2a**, and **2b** can be affected by controlling the temperature of their acetone solutions, whereas dissolving complex **1** in CH_3CN generates complex **3** (vide infra).

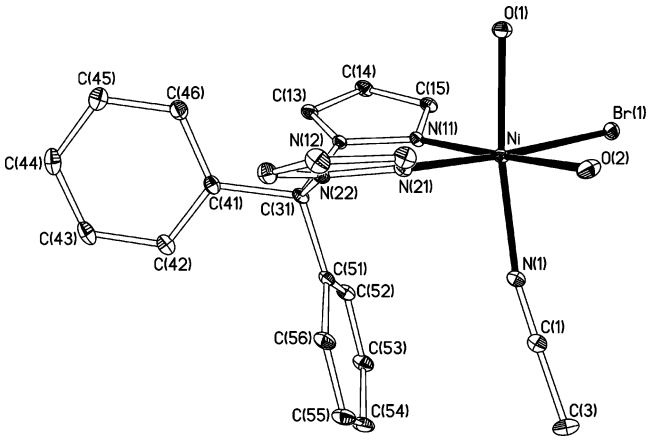

Figure 4. ORTEP view of complex **3**. Thermal ellipsoids are shown at 30% probability. The Br^- counterion has been omitted for clarity.

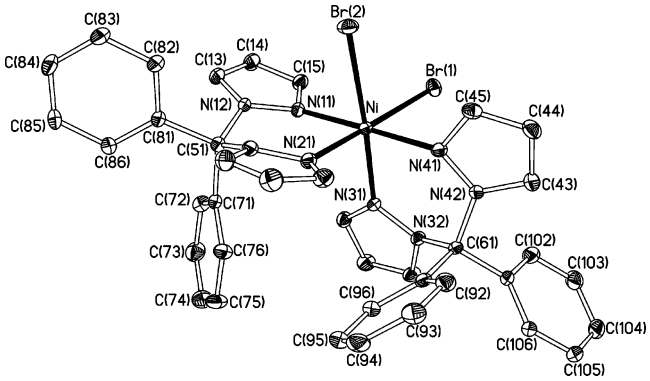

Figure 5. ORTEP view of complex **4**. Thermal ellipsoids are shown at 30% probability.

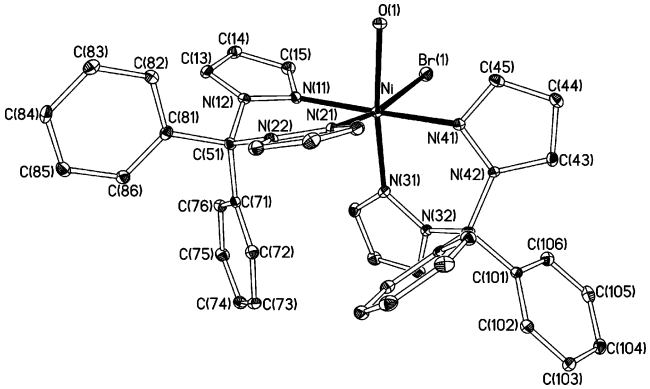

Figure 6. ORTEP view of complex **5**. Thermal ellipsoids are shown at 30% probability. The Br^- counterion has been omitted for clarity.

Formation of the pentacoordinated compounds **1**, **2a**, and **2b** from the 1:1 reactions with $NiBr_2$ is in contrast to the exclusive formation of octahedral products from the 1:1 reactions of $Ni(NO_3)_2$ with dpdpm (cf. (dpdpm)Ni(η^2-NO_3)$_2$, (dpdpm)Ni(η^2-NO_3)(η^1-NO_3)(NCMe).[14] Using a 2:1 dpdpm/$NiBr_2$ ratio gave only octahedral species. Thus, stirring a methanol mixture of $NiBr_2$ and 2 equiv of dpdpm at room temperature and under nitrogen produced a green mixture that was filtered and evaporated to give a green solid; recrystallization of this solid from CH_2Cl_2/Et_2O under a nitrogen atmosphere gave green crystals that were identified by X-ray diffraction studies as the complex **4** (Scheme 3). When complex **4** was exposed to humidity, both in the solid

Table 1. Crystallographic Data for **1**, **2a**, **2b**, and **3**

	1	**2a**	**2b**·H_2O	**3**·CH_3CN
formula	$C_{38}H_{32}N_8Ni_2Br_4$	$C_{19}H_{18}N_4NiBr_2O$	$C_{19}H_{20}N_4NiBr_2O_2$·H_2O	$C_{19}H_{20}N_4Br_2NiO_2$·(C_2H_3N)
M_w	1037.78	536.90	572.94	637.03
cryst color	light brown	green dark	green	green
cryst dimens, mm^3	0.21 × 0.12 × 0.09	0.24 × 0.21 × 0.09	0.46 × 0.23 × 0.15	0.96 × 0.24 × 0.18
symmetry	triclinic	monoclinic	triclinic	triclinic
space group	$P\bar{1}$	$P21/n$	$P\bar{1}$	$P\bar{1}$
a, Å	8.9395(6)	9.8267(5)	10.012(10)	9.41210(10)
b, Å	9.1559(6)	14.4774(7)	10.8995(10)	10.3895(2)
c, Å	11.8205(8)	14.1184(7)	11.3825(10)	14.6092(2)
α, deg	84.166(3)	90	79.529(10)	81.2430(10)
β, deg	81.795(3)	93.890(2)	65.182(10)	79.5330(10)
γ, deg	84.779(3)	90	73.380(10)	66.8230(10)
vol, $Å^3$	949.76(11)	2003.93(17)	1077.589(17)	1286.28(3)
Z	1	4	2	2
D_{calcd}, g cm^{-1}	1.814	1.780	1.766	1.645
diffractometer	Bruker AXS SMART 2K	Bruker AXS SMART 2K	Bruker AXS SMART 2K	Bruker AXS SMART 2K
T, K	100(2)	100(2)	100(2)	100(2)
λ	1.5418	1.5418	1.5418	1.5418
μ, mm^{-1}	6.480	6.203	5.881	4.990
scan type	*ω* scan	*ω* scan	*ω* scan	*ω* scan
F(000)	512	1064	572	640
θ_{max}, (deg)	72.06	72.02	72.84	72.77
h, *k*, *l*	$-11 \le h \le 11$ $-10 \le k \le 11$ $-14 \le l \le 14$	$-12 \le h \le 12$ $-17 \le k \le 17$ $-17 \le l \le 17$	$-12 \le h \le 12$ $-13 \le k \le 12$ $-13 \le l \le 13$	$-11 \le h \le 11$ $-12 \le k \le 13$ $-17 \le l \le 18$
reflns used ($I > 2\sigma(I)$)	3192	3833	4048	4743
abs correction	multiscan SADABS	multiscan SADABS	multiscan SADABS	multiscan SADABS
T (min, max)	0.33, 0.67	0.33, 0.68	0.40, 0.68	0.70, 0.72
R [$F^2 > 2\sigma(F^2)$], R_w (F^2, all)	0.0499, 0.1566	0.0327, 0.0837	0.0288, 0.0753	0.0303, 0.0763
GOF	1.127	1.071	1.102	1.071

state and in solution, it hydrolyzed readily to its mono(aquo) derivative, the blue complex **5**. Moreover, heating solutions or solid samples of **5** or placing them under vacuum gave back the dibromo species **4**. Longer exposures of **4** to ambient humidity produced another blue compound that was insoluble and has not been identified.

Solid-State Structures. Suitable crystals of **1**, **2a**, **2b**, **3**, **4**, and **5** for X-ray diffraction studies were obtained by vapor diffusion of Et_2O or hexane into solutions of these complexes in acetone (**1**, **2a**, and **2b**), acetonitrile (**3**), and dichloromethane (**4** and **5**). All six sets of diffraction data resulted in fairly accurate structures for the complexes studied, as reflected in the *R* values of ca. 0.0289−0.0499. The ORTEP diagrams of these complexes are shown in Figures 1−6, crystallographic data are tabulated in Tables 1 and 2, and bond distances and angles are in Tables 3 and 4.

Complex **1** possesses a crystallographically imposed center of symmetry. On the basis of the low value of the structural index *τ* in each complex,[20] the coordination geometry around the Ni centers in **1** (0.17), **2a** (0.02), and **2b** (0.08) can be characterized as lightly distorted square pyramidal. In comparison to **1**, the closely related dimeric species [(bpp)-Ni(μ-Br)Br]$_2$ displays a less distorted square pyramidal structure ($\tau \approx 0.04$),[13] whereas [(bpm*)Ni(μ-Cl)Cl]$_2$ shows a much greater distortion toward a trigonal bipyramidal

Table 2. Crystallographic Data for **4** and **5**

	4·$2CH_2Cl_2$	**5**
formula	$C_{38}H_{32}N_8NiBr_2.2(CH_2Cl_2)$	$C_{38}H_{34}Br_2N_8NiO$
M_w	989.06	837.26
cryst color	green	blue
cryst dimens, mm^3	0.3 × 0.3 × 0.2	0.28 × 0.13 × 0.03
symmetry	orthorhombic	monoclinic
space group	$P212121$	$P21/n$
a, Å	12.8738(5)	13.0397(2)
b, Å	16.6019(7)	16.3398(2)
c, Å	19.5642(8)	16.8061(2)
α, deg	90	90
β, deg	90	107.6370(10)
γ, deg	90	90
vol, $Å^3$	4181.4(3)	3412.49 (8)
Z	4	4
D_{calcd}, g cm^{-1}	1.571	1.630
diffractometer	Bruker AXS SMART 2K	Bruker AXS SMART 2K
T, K	100(2)	100(2)
λ	1.5418	1.5418
μ, mm^{-1}	5.579	3.925
scan type	*ω* scan	*ω* scan
F(000)	1992	1696
θ_{max}, (deg)	72.03	72.93
h, *k*, *l*	$-15 \le h \le 15$ $-20 \le k \le 20$ $-24 \le l \le 24$	$-16 \le h \le 16$ $-19 \le k \le 20$ $-20 \le l \le 20$
reflns used ($I > 2\sigma(I)$)	8071	5030
abs correction	multiscan SADABS	multiscan SADABS
T (min, max)	0.67, 1.00	0.58, 0.92
R [$F^2 > 2\sigma(F^2)$], R_w (F^2, all)	0.0357, 0.0759	0.0383, 0.0941
GOF	1.054	0.925

(20) Addison, A. W.; Rao, T. N.; Reedijk, J; van Rijn, J.; Verschoor, G. C. *J. Chem. Soc., Dalton Trans.* **1984**, 1349. The strcutural index *τ* is determined from the equation $\tau = (\beta - \alpha)/60$, wherein *β* and α are, respectively, the largest basal angles ($\beta > \alpha$). The *τ* values for perfectly square pyramidal and trigonal bipyramidal structures are 0 and 1, respectively.

Chart 1

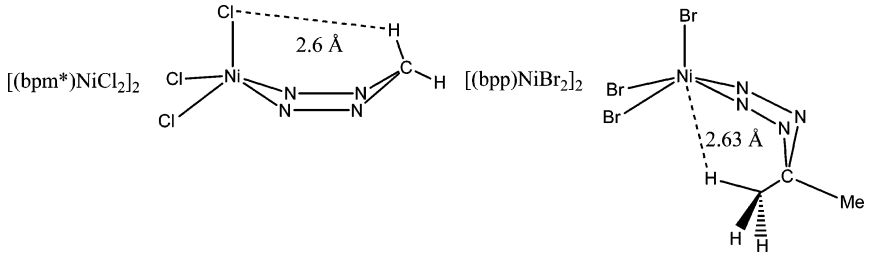

Table 3. Selected Structure Parameters for Complex **1**, **2a**, **2b**, and **3**[a]

	1	**2a**	**2b**	**3**
Ni−Br1	2.4387(7)	2.4595(4)	2.4779(4)	2.5681(4)
Ni−Br2	2.4804(8)	2.4757(4)	−	−
Ni−Br2A	2.5433(8)	−	−	−
Ni−O1	−	2.0571(16)	2.0317(16)	2.0984(15)
Ni−O2	−	−	2.0077(17)	2.0640(15)
Ni−N11	2.047(4)	2.0546(19)	2.0254(18)	2.0766(17)
Ni−N21	2.064(4)	2.0420(19)	2.0316(19)	2.0857(17)
N11−Ni−Br1	100.63(9)	97.61(6)	96.58(5)	94.03(5)
N11−Ni−Br2	155.82(10)	161.93(6)	−	−
N21−Ni−Br1	93.62(10)	100.06(5)	96.79(5)	175.49(5)
N21−Ni−Br2	92.36(10)	94.00(6)	−	−
N11−Ni−N21	85.44(14)	83.83(8)	87.87(7)	86.31(6)
N11−Ni− O1	−	85.67(7)	91.87(7)	89.05(6)
N11−Ni− O2	−	−	161.39(8)	174.83(7)
N21−Ni−O1	−	160.72(7)	165.91(7)	88.76(6)
N21−Ni− O2	−	−	89.75(8)	89.43(7)
N11−Ni− Br2A	90.29(10)	−	−	−
N21−Ni− Br2A	166.07(10)	−	−	−
O1−Ni−Br1	−	97.33(5)	97.24(5)	86.75(4)
O1−Ni−Br2	−	90.98(5)	−	−
O2−Ni−Br1	−	−	102.02(7)	89.98(5)
O1−Ni−O2	−	−	86.00(7)	87.92(7)
Br1−Ni−Br2	103.55(3)	100.430(1)	−	−
Br1−Ni−Br2A	100.21(3)	−	−	−
Br2−Ni−Br2A	86.11(2)	−	−	−
Ni−Br2−NiA	93.89(2)	−	−	−
Ni−N1	−	−	−	2.0957(17)
N11−Ni−N1	−	−	−	99.52(7)
N21−Ni−N1	−	−	−	93.53(6)
N1−Ni−Br1	−	−	−	90.85(5)
N1−Ni−O1	−	−	−	171.25(7)
N1−Ni−O2	−	−	−	83.66(7)

[a] Bond lengths in Å and bond angles in deg.

geometry ($\tau \approx 0.50$).[9j,21] The differences in the overall geometry of the Ni centers in these closely analogous pentacoordinated Ni(II) complexes based on bpm*, bpp, or dpdpm are caused by the differences in the ligand structures, i.e., the different substituents at the 3- and 5-positions of the pyrazolyl groups (H, Me) and the different CR_2 moieties bridging them (R = Ph, Me, H). It is also interesting to note that the axial site in all complexes adopting lightly distorted square pyramidal structures (**1**, **2a**, **2b**, and [(bpp)Ni(μ-Br)-Br]$_2$) is occupied by a Br atom, whereas in the compound [(bpm*)Ni(μ-Cl)Cl]$_2$ that shows major trigonal distortions the axial site is occupied by the pyrazolyl N. This may, of course, be related to the substantial difference in the relative sizes of Cl and Br atoms.[22]

(21) A number of other dinickel species with similar structural motifs have also been reported, including [(dab)NiBr$_2$]$_2$ (dab = *N*,*N*′-di-*t*-butyldiazabutadiene; $\tau \approx 0.12$; Jameson, G. B.; Oswald, H. R.; Beer, H. R. *J. Am. Chem. Soc.* **1984**, *106*, 1669) and [(dmp)NiBr$_2$]$_2$ (dmp = bis(2,9-dimethyl-1,10-phenanthroline; $\tau \approx 0.40$; Butcher, R. J.; Sinn, E. *Inorg. Chem.* **1977**, *16*, 2334).

(22) The authors thank one of the reviewers of the manuscript for this suggestion.

Table 4. Selected Structure Parameters for Complex **4** and **5**[a]

	4 (X2 = Br2)	**5** (X2 = O1)
Ni−Br1	2.5971(4)	2.6146(7)
Ni−X2	2.6476(4)	2.106(2)
Ni−N11	2.0740(19)	2.116(3)
Ni−N21	2.0949(19)	2.074(3)
Ni−N31	2.1031(17)	2.061(3)
Ni−N41	2.0835(18)	2.076(3)
N11−Ni−N21	87.84(7)	84.49(11)
N11−Ni−N31	91.74(7)	95.84(11)
N11−Ni−N41	178.34(7)	176.84(11)
N21−Ni−N31	93.41(7)	100.39(11)
N21−Ni−N41	92.76(7)	93.16(11)
N31−Ni−N41	86.69(7)	86.65(11)
N11−Ni−Br1	94.94(5)	94.26(8)
N21−Ni−Br1	175.74(6)	169.51(8)
N31−Ni−Br1	89.73(5)	90.10(8)
N41−Ni−Br1	84.55(5)	87.67(8)
N11−Ni−X2	86.05(5)	88.56(10)
N21−Ni−X2	84.13(5)	87.23(10)
N31−Ni−X2	176.75(5)	171.52(11)
N41−Ni−X2	95.54(5)	89.22(10)
X1−Ni−X2	92.827(13)	82.33(7)

[a] Bond lengths in Å and bond angles in deg.

The differences in the ligand architecture also give rise to a different conformation of the metallacycle formed by the chelating bis(pyrazole) moiety in the pentacoordinated species. Thus, the methylene moiety displays a Cl···H−C interaction in [(bpm*)Ni(μ-Cl)Cl]$_2$ and an agostic-type Ni···H−C interaction in [(bpp)Ni(μ-Br)Br]$_2$ (Chart 1). The bridging CR_2 moiety in our dpdpm compounds **1**, **2a**, and **2b** points toward the Ni center (Figure 7) to allow a long-range interaction between a C=C bond of a Ph substituent and the Ni center with the following Ni−C distances (in Å): 3.34 and 3.63 in **1**, 3.04 and 3.13 in **2a**, 3.02 and 3.23 in **2b**. An examination of space-filling representations of the solid-state structures of these complexes indicates that steric considerations alone can justify the longer Ni−Ph distances in the dimeric species **1**.[22]

Complexes **3**, **4**, and **5** display slightly distorted octahedral geometries, the cis and trans bond angles are in the range 84−100° and 171−176° in **3**, 84−96° and 176−178° in **4**, and 82−100° and 170−177° in **5** (Tables 3 and 4). An important structural difference between these octahedral species and the above-discussed pentacoordinated compounds is the conformation of the 6-membered ring formed by the coordination of the chelating dpdpm ligand to the Ni center. Evidently, the occupation of the sixth coordination site around the Ni center in the octahedral compounds pushes the Ph substituents of dpdpm toward the equatorial plane, thereby changing the conformation of the Ni−N−N−C−N−N ring from a boat conformation observed in the

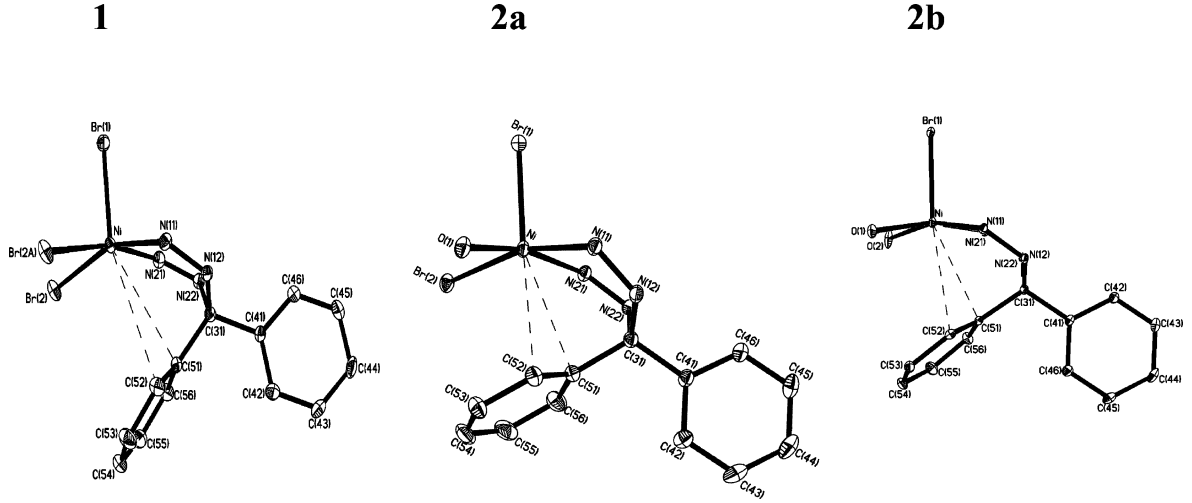

Figure 7. Different perspectives of the ORTEP diagrams for complexes **1**, **2a**, and **2b** showing the long-range Ni−C distances.

pentacoordinated complexes to a half-chair conformation observed in **3**, **4**, and **5**. The different spatial disposition of the Ph substituents in the octahedral and pentacoordinated complexes can be quantified by comparing the angles between the equatorial coordination plane (defined by the ligating atoms N11, N21, Br/O/N, Br/O/N) and the chelation plane defined by the four N atoms of the dpdpm ligand; these angles have the values of ca. 57° in **1**, 47° in **2a**, 38° in **2b**, 4° in **3**, 16° in **4**, and 1° in **5**.

Apart from the overall geometry of the new complexes and the conformation of the metallacycles, the Ni−element bond distances are informative about the relative stabilities of the various species and the relative trans influence of the ligands. For instance, the Ni−(μ-Br) distances in complex **1** are much longer than the axial Ni−Br distance (2.48 and 2.54 vs 2.44 Å, ΔNi−Br > 50 esd). These weak Ni−(μ-Br) interactions explain why this dimer is susceptible to cleavage and transformation into monomeric derivatives **2a** and **2b** by hydrolysis. Fairly inequivalent distances were also found for the Ni−Br bonds in **2a** (axial < basal; ΔNi−Br ≈ 40 esd) and the Ni−O bonds in **2b** (ΔNi−O ≈ 14 esd). On the other hand, the two Ni−N distances in **1**, **2a**, and **2b** are fairly similar to each other (ΔNi−N ≈ 4 esd in **1**, ≈ 6 esd in **2a**, and ≈ 3 esd in **2b**).

Finally, the Ni−N distances trans to Ni−OH_2 are somewhat shorter than the corresponding distances trans to Ni−Br in **2a** (2.042(2) vs 2.055(2) Å), **3** (2.077(2) vs 2.086(2) Å), and **5** (2.061(3) vs 2.074(3) Å), implying that Br has a greater trans influence than H_2O. Moreover, in **4** the Ni−N_{av} distance trans to Br is somewhat longer than those trans from the pyrazolyl group (2.099(2) vs 2.079(2) Å), implying a slightly greater trans influence for Br. Interestingly, the Ni−O distance trans to MeCN in **3** is longer than that trans to the pyrazolyl group (2.098(2) vs 2.064(2) Å), implying a greater trans influence for MeCN. These observations lead to the following order of relative trans influence strengths in these compounds: $CH_3CN \approx Br > H_2O \approx$ dpdpm. It should be noted, however, that the structural parameters for the octahedral species arising from the reactions of $Ni(NO_3)_2$ with dpdpm have implied a greater trans influence for the pyrazolyl group (dpdpm ≈ $H_2O \approx \eta^1$-$ONO_2 > CH_3CN \approx \eta^2$-$O_2NO$).[14]

Magnetic Measurements and Spectroscopic Studies. Magnetic susceptibility measurements using the Gouy method have established that all the dpdpm compounds investigated here are paramagnetic in the solid state. Thus, μ_{eff} for pentacoordinated complexes **1**, **2a**, and **2b** were found to be between 3.2 and 3.4 μ_B, whereas those of the hexacoordinated complex **3**−**5** were ca. 3.3 μ_B. All of these values are in the expected range for square pyramidal or octahedral Ni(II) complexes having two unpaired electrons.[23]

That the paramagnetism of these compounds is maintained in solution is reflected in ^{1}H NMR spectra displaying broad and, for the most part, featureless signals that resonated as far upfield as −160 ppm and as far downfield as 70 ppm. The broadness of the NMR signals in bis(pyrazolyl)alkane complexes may also be caused by the dynamic exchange process involving the flipping of the M−N−N−C−N−N ring between chair and boat conformations. Moreover, the ^{1}H NMR spectra recorded in CD_3CN feature a fairly broadened residual solvent signal (at 1.94 ppm) in addition to somewhat broader signals due to the dpdpm ligand (at 6.69, 6.36, and 6.13 ppm). We suspect, therefore, that a ligand exchange process involving CD_3CN molecules and the dpdpm ligand might be taking place in solution, but no dpdpm-free complex or species with monodentate dpdpm has been obtained in the solid state. The IR spectra of the new complexes contain a large number of absorptions that serve primarily as fingerprints for this family of complexes.

Solvato- and Thermochromism of the Pentacoordinated Species. The presence of an "unfilled" coordination site around the Ni center in the pentacoordinated complexes **1**, **2a**, and **2b** facilitates the interaction of these species with nucleophiles or coordinating counterions. We have examined the interaction of these complexes with solvent molecules of varying nucleophilicities and found a number of interesting color changes that signal structural changes. Since temper-

(23) Collinson, S. R.; Schröder, M. Nickel: Inorganic and Coordination Chemistry. In *Encyclopedia of Inorganic Chemistry*, 2nd ed.; King, R. B., Ed.; Wiley InterScience: Chichester, 2005; Vol. VI.

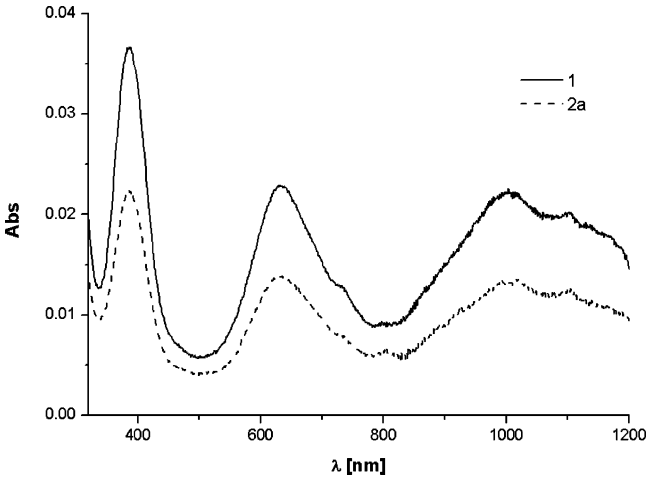

Figure 8. Room-temperature UV−vis−NIR spectra of MeOH solutions of **1** (1.3 mM) and **2a** (2.1 mM).

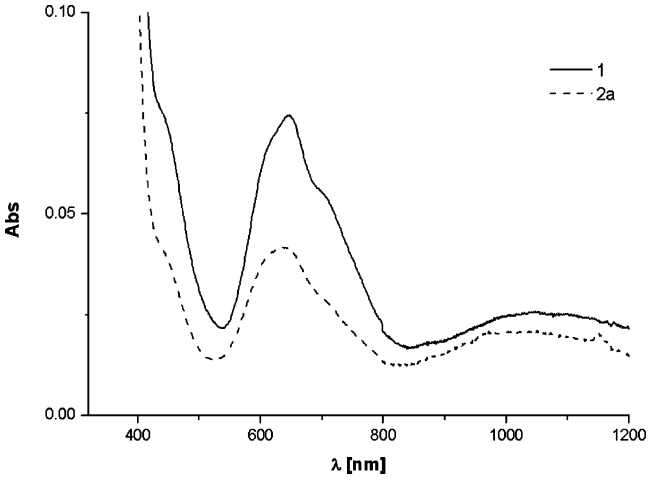

Figure 9. Room-temperature UV−vis−NIR spectra of CH_3CN solutions of **1** (1.3 mM) and **2a** (2.7 mM).

ature variations can also influence metal−ligand interactions and structural changes, we have also probed the influence of temperature on the optical properties of these compounds. Given the similarities of the UV−vis−NIR spectra for solutions of **2a** and **2b** in various solvents, we have focused the present discussion on the spectra for **1** and **2a** only.

Figures 8 and 9 show the UV−vis−NIR spectra of **1** and **2a** in MeOH (blue) and CH_3CN (lime green), respectively. It is noteworthy that these spectra display the characteristic spectral pattern for octahedral Ni(II) compounds. Thus, all of these spectra contain the allowed d−d transitions $^3A_{2g} \rightarrow {}^3T_{2g}$, $^3A_{2g} \rightarrow {}^3T_{1g}(^3F)$, and $^3A_{2g} \rightarrow {}^3T_{1g}$ (^3P),[24] although the bands of the CH_3CN spectra are more intense. Interestingly, the middle bands in these spectra ($^3A_{2g} \rightarrow {}^3T_{1g}$) have multiple maxima that arise from interactions between the allowed and nonallowed excited states, as described elsewhere.[25]

The pair wise similarities of the spectra obtained for MeOH and CH_3CN solutions of **1** and **2a** indicate that these compounds have similar structures in these solvents. Indeed, comparison of the CH_3CN spectra to that of complex **3** in this solvent shows that acetonitrile solutions of **1**, **2a**, and **3** contain the same species. We conclude, therefore, that interaction of the Ni center in **1** or **2a** with acetonitrile involves the coordination of CH_3CN and H_2O to form **3**. In the case of the species generated in MeOH solutions of **1** and **2a**, the absence of reliable structural information does not allow us to determine whether the resulting octahedral species is a simple MeOH or water adduct[26,27] or a compound arising from the displacement of Br by MeOH or water.[28]

Heating the MeOH solution of **1** produced a color change, going from light blue at room temperature to light green at ca. 60 °C, but the spectra recorded for these solutions do not show significant changes in the shapes of the bands or the energy maxima (<5−10 nm). These color changes are likely due to ligand exchange reactions that cause only minor modifications in the overall geometry of the complex.

The electronic spectra of **2a** in CH_2Cl_2 and acetone (Figure 10) were quite different from those discussed above. For instance, the room-temperature spectrum recorded for the acetone solution showed four main bands at 488, 650, 861, and 1006 nm; the band at 650 nm features a shoulder at 712 nm. The room-temperature spectrum recorded in CH_2Cl_2 also shows four main peaks at 491, 662, 859, and 1002 nm; the band at 491 nm also shows a shoulder at 560 nm. These spectra are quite similar, their main difference being the position of the shoulder band. These observations indicate that CH_2Cl_2 and acetone solutions of **2a** do not contain octahedral species. Literature reports show that most pentacoordinated Ni(II) species display three or four bands of variable intensities.[29] On the other hand, computational studies have indicated that Ni(II) compounds surrounded by

(24) (a) Landry-Hum, J.; Bussière, G.; Daniel, C.; Reber, C. *Inorg. Chem.* **2001**, *40*, 2595. (b) Bussière, G.; Beaulac, R.; Cardinal-David, B.; Reber, C. *Coord. Chem. Rev.* **2001**, *219*−*221*, 509.

(25) Very similar "weak shoulders" have been observed in the absorption spectra of many octahedral Ni(II) complexes, including $[Ni(NH_3)_6]^{2+}$. For a discussion of this phenomenon, including detailed analyses of these transitions based on Tanabe−Sugano diagrams and modern theoretical models, see : (a) Bussière, G.; Reber, C. *J. Am. Chem. Soc.* **1998**, *120*, 6306. (b) Triest, M.; Bussière, G.; Bélisle, H.; Reber, C. *J. Chem. Ed.* **2000**, *77*, 670. Available at http://jchemed.chem.wisc.edu/jcewww/articles/JCENi/JCENi.html. (c) Bussière, G.; Reber, C.; Neuhauser, D.; Walter, D. A.; Zink, J. I. *J. Phys. Chem. A* **2003**, *107*, 1258. (d) Nolet, M.-C.; Beaulac, R.; Boulanger, A.-M.; Reber, C. *Struc. Bonding* **2004**, *107*, 145. (e) González, e.; Rodrigue-Witchel, A.; Reber, C. *Coord. Chem. Rev.* **2007**, *251*, 351.

(26) For a few recent reports on a variety of Ni(II) complexes of (N−N) donor ligands containing coordinated MeOH see: (a) Sun, Y.-J; Cheng, P.; Yan, S.-P; Jiang, Z.-H; Liao, D.-Z; Shen, P.-W. *Inorg. Chem. Comm.* **2000**, *3*, 289. (b) Dorta, R.; Shimon, L. J. W.; Rozenberg, H.; Ben-David, Y.; Milstein, D. *Inorg. Chem.* **2003**, *42*, 3160. (c) Casabó, J.; Pons, J.; Siddiqi, K. S.; Teixidor, F.; Molins, E.; Miravitlles, C. *J. Chem. Soc., Dalton Trans.* **1989**, 1401. (d) Makowska-Crzyska, M. M.; Szajna, E.; Shipley, C.; Arif, A. M.; Mitchell, M. H.; Halfen, J. A.; Berreau, L. M. *Inorg. Chem.* **2003**, *42*, 7472.

(27) Examples of penta- and hexacoordinated Ni(II) complexes with a coordinated water molecule: (a) Adams, H.; Clunas, S.; Fenton, D. E. *Acta Crystallogr*. **2004**, *E60*, m338. (b) Matecka, M.; Rybarczyk-Pirek, A.; Olszak, T. A.; Malinowska, K.; Ochocki, J. *Acta Crystallogr*. **2001**, *C57*, 513. (d) Bazzicalupi, C.; Bencini, A.; Duce, C.; Fornasari, P.; Giorgi, C.; Paoletti, P.; Pardini, R.; Tinè, M. R.; Valtancoli, B. *Dalton Trans*. **2004**, 463.

(28) It should be recalled, however, that the only crystals obtained from blue solutions of **2a** in MeOH are those of light green **2b**, implying that the octahedral species present in these solutions is a more soluble, presumably neutral compound such as $[(dpdpm)NiBr_2(OH_2)(L)]$ (L = H_2O or MeOH).

(29) (a) Larue, B.; Tran, L.-T.; Luneau, D.; Reber, C. *Can. J. Chem.* **2003**, *81*, 1168. (b) Sacconi, L.; Nannelli, P.; Nardi, N.; Campigli, U. *Inorg. Chem*. **1965**, *4*, 943.

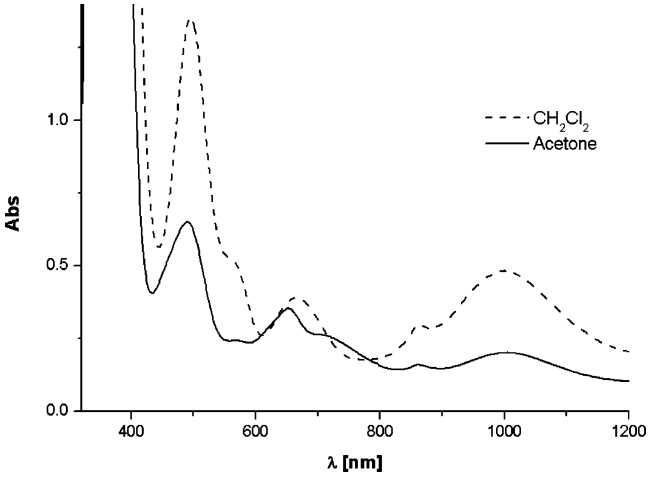

Figure 10. Room-temperature UV−vis−NIR spectra of **2a** in CH_2Cl_2 (8.7 mM) and acetone (8.3 mM).

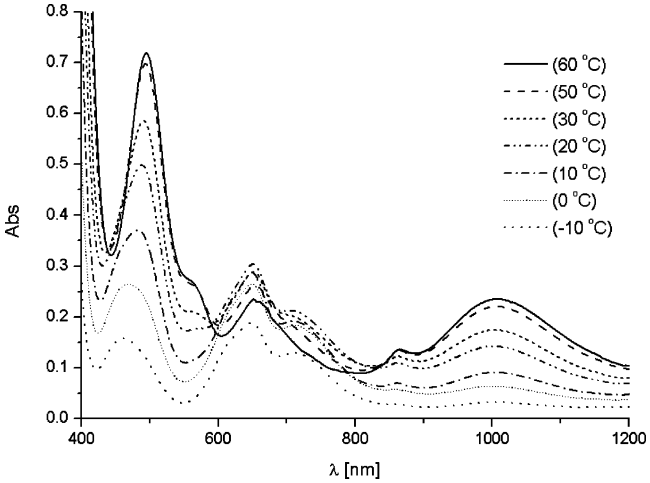

Figure 11. Variable-temperature UV−vis−NIR spectra for a 6.5 mM solution of **2a** in acetone.

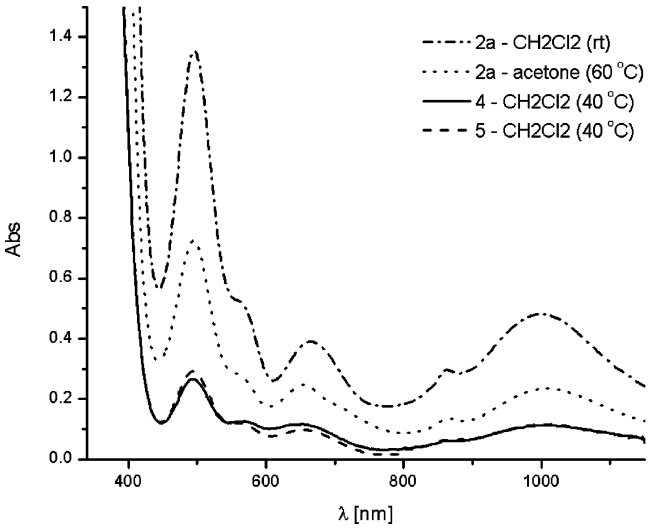

Figure 12. UV−vis−NIR spectra for solutions of **2a** (8.7 mM in CH_2Cl_2 and 6.5 mM in acetone) and acetone solutions of **4** (4.7 mM) and **5** (6.6 mM).

weak-field ligands arranged in a square pyramidal geometry (C_{4v} idealized symmetry, high-spin) should give rise to six spin-allowed transitions in the UV−vis region.[30] We propose that our observations are consistent with the maintenance of square pyramidal structure for **2a** in acetone and CH_2Cl_2 solutions, which is reasonable because both of these solvents have weaker coordinating abilities relative to MeOH and CH_3CN.

The colors of the acetone and CH_2Cl_2 solutions of **2a** and their temperature-dependence also reveal an interesting interconversion between **2a** and **1**. Thus, the CH_2Cl_2 solution of **2a** is brown, very similar to the color of solid samples of **1**, while the room-temperature acetone solution of **2a** is green. Varying the temperature of the acetone solution of **2a** caused a color variation from light green (<30 °C) to dark green (30−40 °C) to brown (40−60 °C). Cooling the samples to 18 °C regenerated the light green color of the solution, and repeating this heating−cooling cycle eight times produced the same observations. The variable-temperature spectra of an acetone solution of **2a** showed a continuous blue-shift of the shoulder band from ca. 711 nm at −10 °C to ca. 555 nm at 60 °C (Figure 11). It is noteworthy that the high temperature acetone spectrum is virtually identical to the room-temperature CH_2Cl_2 spectrum of **2a** (Figure 12), and both of these solutions have the same color as the solid samples of **1**. Since **1** can be prepared by dehydration of **2a** or **2b** (vide supra), these observations suggest that the continuous and reversible thermochromism of **2a** in acetone involves its conversion to **1** at high temperatures. Conversion of complex **2a** to **1** can also occur at room temperature in concentrated CH_2Cl_2 solutions. Unfortunately, the insufficient solubility of **1** in CH_2Cl_2 and acetone prevented us from recording the spectra of **1** in these solvents, which would allow us to confirm the conversion of **1** to **2a**.

Finally, we have briefly studied the effect of solvent vapor on the pentacoordinated species **2a** and **2b**. These studies showed that **2b** is readily converted to **1** in the presence of solvent vapors, whereas **2a** did not register important changes. Thus, exposing a small light green crystal of **2b** to the vapors of benzene, Et_2O, or toluene turned the crystals to brown in less than 2 min. Visual inspection indicated that the sample had lost its crystallinity; however, exposing this brown sample to humidity changed it back to green in a very slow process (many days).

Solvato- and Thermochromism of the Octahedral Species 4 and 5. In order to determine whether the coordinatively saturated Ni centers in our octahedral species can undergo similar solvato- and thermochromic changes, we examined (visually and by spectroscopy) the colors of the solutions of the bis(dpdpm) compounds **4** and **5**. Since complex **4** (green) is readily converted to **5** (blue) in the presence of humidity, both in solution and solid state, the thermo- and solvatochromism tests were carried out using dried and distilled solvents and with freshly grown crystals of these complexes.

Complexes **4** and **5** give variously colored solutions in different solvents; in addition, some of these solutions changed color as a function of temperature. Thus, CH_2Cl_2 solutions of **4** are dark green at room temperature and pink at 40 °C. The MeOH solution of **4** turns from turquoise blue

(30) Ciampolini, M. *Inorg. Chem.* **1966**, *5*, 35.

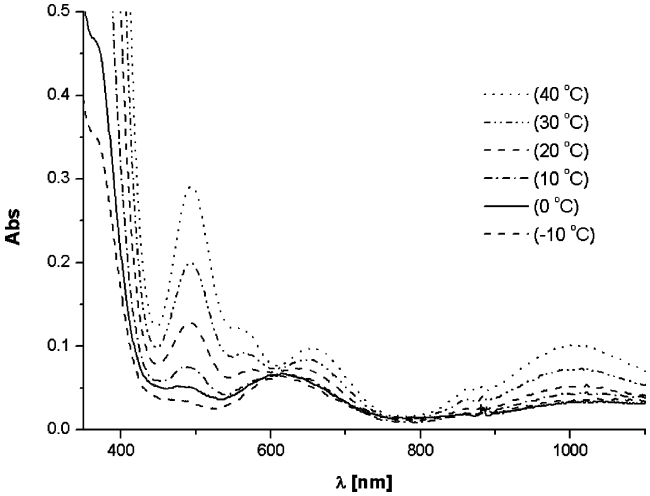

Figure 13. Variable-temperature UV−vis−NIR spectra for **4** in CH_2Cl_2 (4.7 mM).

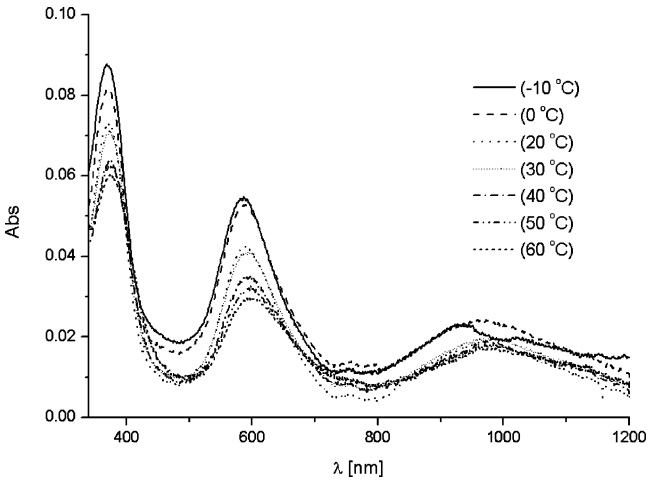

Figure 14. Variable-temperature UV−vis−NIR spectra for **4** in MeOH (3.9 mM).

at 20 °C to light green at 60 °C. The CH_3CN solutions of **4** are light green at room temperature or below, becoming dark green at higher temperatures. Room-temperature solutions of complex **5** were light blue in both CH_2Cl_2 and MeOH but green in CH_3CN. Increasing the temperature turned the CH_2Cl_2 solution from blue to pink at 40 °C, whereas the MeOH and CH_3CN solutions did not change color upon heating.

The UV−vis−NIR spectra of various solutions prepared from crystals of **4** and **5** were recorded to monitor spectral changes as a function of solvent and temperature. Figures 13−15 show the variable-temperature spectra of **4** in CH_2Cl_2, MeOH, and CH_3CN, respectively. Figure 16 shows the variable temperature spectra recorded for CH_2Cl_2 solution of **5** (6.6 mM); the MeOH and CH_3CN spectra were very similar to those of complex **4**. The spectra taken at 20 °C for MeOH and CH_3CN solutions of complex **4** show the expected pattern for octahedral species, implying that **4** generates fairly similar species in these relatively nucleophilic solvents. Varying the temperature of the MeOH solutions from −10 to 60 °C caused a red-shift of the 586 nm band (to 599 nm, Figure 14), whereas the corresponding band in the CH_3CN spectra (Figure 15) showed a blue-shift (591 to

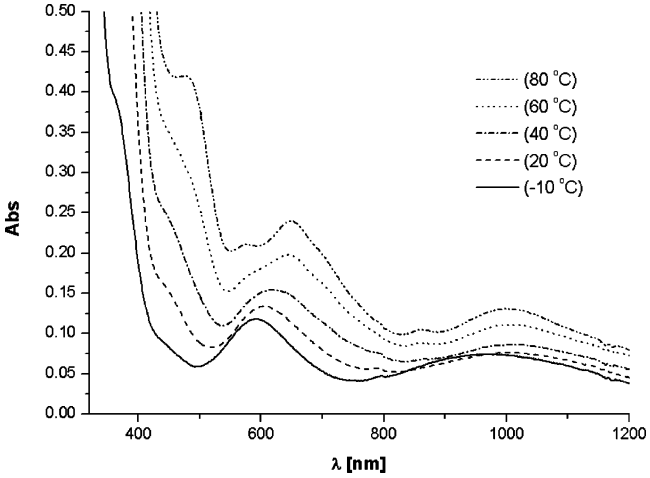

Figure 15. Variable-temperature UV−vis−NIR spectra for **4** in CH_3CN (8.7 mM).

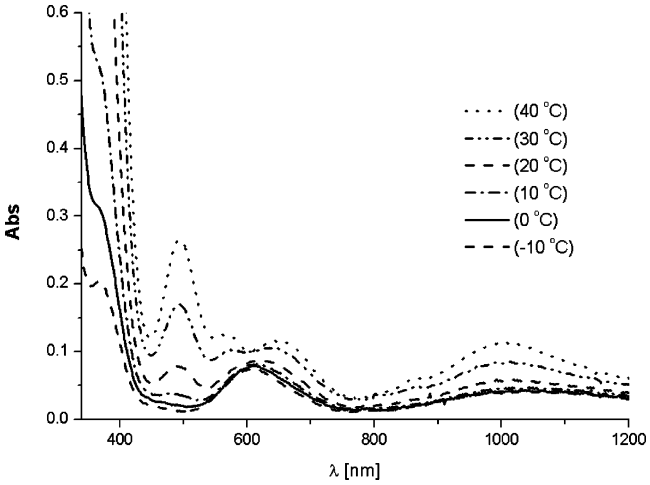

Figure 16. Variable-temperature UV−vis−NIR spectra for **5** in CH_2Cl_2 (6.6 mM).

577 nm) in addition to the emergence of a new shoulder band at 575 nm.

The variable-temperature spectra of **4** and **5** in CH_2Cl_2 (Figures 13 and 16) registered major changes over a much narrower range of temperature (−10 to +40 °C), implying that significant changes take place in the overall structure of these complexes. It is interesting to note the striking similarity between the −10 and 40 °C spectra of **4** and **5**. Furthermore, as was mentioned above, at 40 °C the spectral features are reminiscent of those observed for CH_2Cl_2 solution of complex **2a** at room temperature and those of the acetone solution at high temperatures. On the basis of these observations, we propose that heating CH_2Cl_2 solutions of the octahedral, bis(dpdpm) complexes **4** and **5** leads to the dissociation of a dpdpm ligand to form mono(dpdpm) species. The similarity between the colors of these solutions and the solid sample of **1** points to the possible formation of the dimeric structure of **1** in high-temperature solutions of **4** and **5**.

Conclusion

$NiBr_2$ forms pentacoordinated complexes when it is reacted with 1 equiv of dpdpm in weakly coordinating solvents. This

is in contrast to the exclusive formation of octahedral species from the reaction of $Ni(NO_3)_3$ under similar conditions. The unusual geometry of the $NiBr_2$ derivatives appears to be stabilized, in the solid state, by long-range Ni−Ph interactions. In contrast, reactions using a 1:2 Ni/dpdpm ratio give octahedral species with both nitrate and bromide derivatives.

A common aspect of all Ni−dpdpm complexes prepared to date is the lability of all Ni−ligand bonds. This is perhaps the reason why these compounds are not suitable precursors for organometallic derivatives. It is worth noting, however, that the facile dissociation of Br^- or NO_3^- bestows interesting solvato-, vapo-, and thermochromic properties to these compounds. The results of our studies encourage us to explore the potential of these complexes in detecting solvent vapors or anions.

Experimental Section

General. The main ligand used in this study, dpdpm, was synthesized according to a published procedure.[19] Anhydrous $NiBr_2$ was purchased from Sigma-Aldrich, stored in a drybox, and used without further dehydration. Where necessary, the synthetic manipulations were carried out in dry and oxygen-free solvents under an atmosphere of ultrahigh purity nitrogen using standard Schlenk techniques and a drybox. The elemental analyses (C, H, and N) were performed in duplicate by Laboratoire d'Analyse Élémentaire de l'Université de Montréal. The ^{1}H NMR spectra were recorded on a Bruker Av400 (at 400 MHz). The IR spectra were recorded between 4000 and 400 cm^{-1} using KBr pellets on a Perkin-Elmer Spectrum One spectrophotometer using the Spectrum v.3.01.00 software. The UV−vis−NIR spectra were recorded between 1300 and 250 nm with a 1 cm quartz cell on a Varian Cary 500i; the variable-temperature spectra were recorded on a Cary 500 spectrophotometer. The magnetic susceptibility measurements were carried out at room temperature using the Gouy method with a Johnson Matthey magnetic susceptibility balance, using $HgCo(NCS)_4$ as standard.

Syntheses. [(dpdpm)Ni(μ-Br)Br]$_2$ (1). A solution of dpdpm (1.00 g, 3.33 mmol) in distilled acetone (25 mL) was added to a stirred suspension of $NiBr_2$ (0.75 g, 3.34 mmol) in distilled acetone (25 mL). The reaction mixture was heated to reflux for 18 h, cooled to room temperature, and filtered, and the remaining solid was washed with Et_2O (3 × 20 mL) to give an orange-brown powder (1.30 g, 79% crude yield). X-ray quality single crystals (brown) were obtained by slow diffusion of Et_2O into a concentrated acetone solution kept at room temperature. mp = 260 °C. μ_{eff} = 3.55 μ_B. Anal. Calcd for $[C_{19}H_{16}N_4NiBr_2]_2$: C, 43.98; H, 3.11; N, 10.80. Found: C, 43.58; H, 2.99; N, 10.78%. ^{1}H NMR (CD_3OD): 59.55 (br), 40.47 (br), 7.58 (br), 7.47−7.44 (br), 7.34 (br), 7.37 (br), 7.18 (br), 6.72 (br), 2.144(s), −141.07(br), −160.34 ppm (br). IR (KBr, cm^{-1}): 3604 (s), 3392 (br), 3158 (m), 3118 (m), 3058 (m), 1631 (m), 1517 (m), 1491 (s), 1450 (s), 1437 (s), 1408 (s), 1385 (s), 1330 (m), 1313 (vs), 1253 (s), 1222 (s), 1199 (s), 1171 (m), 1098 (s), 1080 (s), 1074 (s),()w,999 (m), 940 (w),924 (w), 918 (m), 891 (m), 870 (m), 853 (m), 776 (s), 754 (vs), 704 (s), 692 (s), 656 (s), 637 (s), 614 (w), 605 (w), 497 (w).

[(dpdpm)NiBr$_2$(H$_2$O)] (2a). A solution of dpdpm (0.50 g, 1.66 mmol) in methanol (30 mL) was added to a stirred suspension of $NiBr_2$ (0.36 g, 1.66 mmol) in (30 mL) methanol. The reaction mixture was stirred for 20 h at room temperature, filtered to remove unreacted $NiBr_2$, and evaporated to give a dark green powder (2.99 g, 83% crude yield). X-ray quality single crystals (dark green) were obtained by slow diffusion of Et_2O into a concentrated acetone solution kept at room temperature. mp = 234 °C. μ_{eff} = 3.21 μ_B. Anal. Calcd for $C_{19}H_{18}N_4O_1NiBr_2$: C, 42.51; H, 3.38; N, 10.44. Found: C, 42.96; H, 3.35; N, 10.28%.^{1}H NMR ($CDCl_3$): 69.86 (br), 50.42 (br), 37.94 (br), 6.62 (br), 5.65 (br), 4.45 (br), 3.92 (br), 3.12 (br), 2.2 (br), 1.47 (br) 1.30 (br) 0.089 (br) −130.7 (br) −150.34 (br), −163.01 ppm (br). IR (KBr, cm^{-1}): 3323 (br), 3150−3033 (w), 1631 (vs), 1516 (w), 1491 (m), 1451 (s), 1434 (m), 1406 (s), 1385(m), 1332 (m), 1314 (s), 1254 (m), 1226 (m), 1198 (s), 1171 (m), 1091 (w), 1080 (w), 1070 (vs), 999 (m), 942 (w), 923 (m), 890 (m),867 (m), 847 (w), 771 (vs), 775 (s), 699 (s), 657 (m), 638(m), 605 (m), 578 (w), 502 (w).

[(dpdpm)NiBr(H$_2$O)$_2$]Br (2b). The procedure used for the synthesis of **2a** was followed. X-ray quality single crystals (light green) were obtained by slow diffusion of hexane into a concentrated acetone solution kept at room temperature. mp > 260 °C. μ_{eff} = 3.22 μ_B. Anal. Calcd for $C_{19}H_{20}N_4O_2NiBr_2$: C, 41.13; H, 3.63; N, 10.10. Found: C, 40.63; H, 3.43; N, 9.83%. ^{1}H NMR (CD_3OD): 60.81 (br), 39.05 (br), 7.28 (br), 7.12 (br), 6.72 (br), −140.55 (br), −162 ppm (br). IR (KBr, cm^{-1}): 3395 (br), 3344 (br), 3127−3056 (w), 1631 (s), 1516 (m), 1491 (m), 1450 (s), 1437 (m), 1414 (s), 1385 (m), 1336 (m), 1318 (s), 1257 (m), 1223 (w), 1214 (m), 1198 (m), 1185 (w), 1174 (w), 1104 (m), 1086 (m), 1069 (vs), 1001 (m), 942 (w), 922 (m), 891 (m), 870 (w), 843 (w), 780 (s), 757 (w), 749 (vs), 702 (s), 567 (w), 642 (w), 611 (w), 600 (w), 537 (w), 511 (w).

[(dpdpm)NiBr(H$_2$O)$_2$(CH$_3$CN)]Br (3). A solution of dpdpm (2.00 g, 6.66 mmol) in acetonitrile (30 mL) was added to a stirred suspension of $NiBr_2$ (1.46 g, 6.70 mmol) in acetonitrile (30 mL). The reaction mixture was stirred for 20 h at room temperature, filtered, and the filtrate was evaporated to give a green solid (3.35 g, 85% crude yield). X-ray quality single crystals of **3** (green) were obtained by slow diffusion of hexane into a concentrated solution of acetonitrile kept at room temperature. mp = 229 °C. μ_{eff} = 3.33 μ_B. Anal. Calcd for $C_{21}H_{23}N_5O_2NiBr_2 \cdot CH_3CN$: C, 43.37; H, 4.11; N 13.19. Found: C, 42.99; H, 4.07; N, 12.91%. ^{1}H NMR (CD_3CN): 70.97 (br), 61.54 (br), 43.75 (br), 39.20 (br), 7.51−7.43, 6.53-(br), 5.70 (br), 5.51(br), −129.97, −140.22 (br), −157.02 (br), −161.82 ppm (br). IR: 3605 (s), 3392 (br), 2368−2241 (w), 1644 (br), 1515 (m), 1491(s), 1450 (s), 1438 (s), 1410 (s), 1384 (s), 1332 (w), 1309 (vs), 1252 (m), 1218 (s), 1193 (s), 1166 (m), 1109 (s), 1078 (m), 1067 (vs), 1031 (w), 1000 (m), 940 (w), 918 (m), 892 (m), 874 (m), 858 (w), 784 (s), 764 (vs), 754 (vs), 704 (s), 568 (w), 658 (w), 636 (m), 614 (w),724 (w), 604 (m), 504 (m).

[(dpdpm)$_2$NiBr$_2$] (4) and [(dpdpm)$_2$NiBr(H$_2$O)]Br (5). A solution of dpdpm (0.50 g, 1.66 mmol) in distilled hot methanol (20 mL) was added to a stirred suspension of $NiBr_2$ (0.18 g, 0.82 mmol) in distilled methanol (15 mL). The reaction mixture was stirred for 20 h at room temperature under nitrogen, filtered, and the filtrate evaporated to give a green solid (0.56 g, 81% crude yield). X-ray quality single crystals of **4** (green) were obtained by slow diffusion of Et_2O into a concentrated (green) solution of CH_2Cl_2 kept at room temperature and under nitrogen. Alternatively, repeating this same recrystallization procedure but with the solution exposed to air gave blue crystals of **5**. The latter were also obtained by exposing the green crystals of **4** to ambient atmosphere overnight. **4**: mp = 120 °C. μ_{eff} = 3.26 μ_B. Anal. Calcd for $C_{38}H_{34}N_8$ Ni $Br_2 \cdot CH_2Cl_2$: C, 51.81; H, 3.79; N, 12.39. Found: C, 51.60; H, 3.26; N, 12.25%. ^{1}H NMR ($CDCl_3$): 60.33 (br), 38.75 (br), 7.18 (br), −141.05 (br), −162.17 ppm (br). IR: 3430 (br), 3146 (m), 3110 (m), 3098 (m), 3062 (m), 2962 (m), 2925 (m), 2855 (m), 2377 (w), 1629 (br), 1513 (m), 1491 (s), 1450 (s), 1433

(s), 1404 (m), 1382 (m), 1303 (s), 1272 (w), 1250 (w), 1222 (m), 1189 (s), 1161 (m), 1106 (s), 1085 (m), 1066 (vs), 1000 (w), 979 (w), 938 (m), 915 (m), 889 (m), 872 (w), 788 (w), 754 (vs), 725 (s), 699 (s), 669 (w) 658 (m), 634 (m), 605 cm^{-1} (w). **5**: mp = 120 °C. μ_{eff} = 3.01 μ_B. Anal. Calcd for $C_{38}H_{34}N_8O_1NiBr_2$: C, 54.51; H, 4.09; N, 13.38. Found: C, 54.51; H, 3.97; N, 13.52%. ^1H NMR ($CDCl_3$): 60.39 (br), 37.79 (br), 7.46 (br), 6.68 (br) −162.99 ppm (br). IR (KBr, cm^{-1}): 3512 (s), 3431 (br), 3104 (m), 3052 (s), 2918 (m), 2850 (m), 2375 (w), 2361 (w), 2347 (w), 2019 (w), 1820 (w), 1763 (w), 1603 (br), 1522 (m), 1516(m), 1491 (s), 1449 (s), 1435 (s), 1411 (m), 1384 (m), 1332 (m), 1305 (s), 1250 (m), 1220 (s), 1193 (s), 1187 (s), 1167 (m), 1108 (s), 1087 (m), 1064 (vs), 1000(w), 990 (w), 980 (w), 938 (w), 918 (m), 914 (m), 890 (m), 873 (m), 856 (w), 762 (vs), 752 (vs), 700 (s), 683 (w), 657 (m), 636 (m), 618 (w), 604 (w).

Crystallographic Studies. All diffraction data sets were collected on a Bruker AXS SMART 2K diffractometer mounted with Cu Kα radiation at 100(2) K (SMART software).[31] Cell refinement and data reduction were carried out using SAINT.[32] All structures were solved by direct methods using SHELXS97,[33] and the refinements were done on F^2 by full-matrix least-squares.[34] All non-hydrogen atoms were refined anisotropically. The positional parameters for H atoms in water molecules were refined isotropically, but all other hydrogens were constrained to the parent atom using a riding model.

The crystal structures of **2a**, **2b**, **3**, and **5** are stabilized by intermolecular hydrogen bonds. The details on O−H···O distances are available from the detailed structure reports. The structure of complex **4** contained two disordered solvent molecules of CH_2Cl_2, which were refined isotropically using a constrained model. Disordered solvent molecules were then introduced over two positions and refined using the ISOR restrained technique. For the sake of clarity, molecules of solvents (in **2b**, **3**, and **4**) and the counterions (in **2b**, **3**, and **5**) have been removed from the ORTEP III[35] diagrams.

All details concerning the refinement of the crystal structures are listed in Tables 1 and 2. The relevant bond distance and angles are tabulated in Tables 3 and 4. Crystallographic data for the structural analysis have been deposited with the Cambridge Crystallographic Data Centre, CCDC No. 633340 (**1**), 633341 (**2a**), 633342 (**2b**), 633343 (**3**), 633344 (**5**), and 633345 (**4**). Copies of this information may be obtained free of charge from The Director, CCDC, 12 Union Road, Cambridge, CB2 1EZ, UK (fax: +44-1223-336-033; email: deposit@ccdc.cam.ac.uk or www: http://www.ccdc.cam.ac.uk).

Testing the Reversible Solvato-, Vapo-, and Thermochromic Behaviors of Complexes 1, 2a, 4, and 5. Dissolving solutions of **2a** (8.2−9.8 mM) gave different colors depending on the solvent and the temperature of the solution. At room temperature, **2a** is dark olive in acetone, forest green in CH_3CN, and light blue in MeOH; the color of the CH_2Cl_2 solutions was concentration-dependent, giving light pink in dilute solutions and brown in concentrated solutions. Evaporation of all these solutions regenerated the green solid **2a**. Moreover, evaporation of concentrated acetone solutions with heating led to the precipitation of a brownish solid identified as **1**. The UV−vis−NIR spectra of these solutions were recorded and are presented in Figures 8−11. The thermochromism of the complexes was studied by recording the variable-temperature UV−vis−NIR spectra (−10 to 60 °C). The spectral features are discussed in the Results and Discussion section.

The UV−vis−NIR spectra for solutions of complexes **4** and **5** were recorded to monitor any spectral changes as a function of solvent and temperature. Figures 13−15 show the variable-temperature spectra of **4** in CH_2Cl_2 (4.7 mM), MeOH (3.9 mM), and CH_3CN (8.7 mM). The sensitivity of complex **4** to humidity required that its spectra be recorded using crystals of **4** that had been kept in a drybox or in a desiccator containing $CaCl_2$ in order to minimize any direct contact with humidity. The variable-temperature spectra recorded for a 6.6 mM CH_2Cl_2 solution of **5** are shown in Figure 16. The thermochromism of **4** and **5** is discussed in the Results and Discussion section.

The vapochromic behavior of **1** and **2b** was studied briefly, as follows. A crystal of **2b** was fixed onto a glass fiber attached to the inside of the cap for a 5 mL drum vial. The cap was then placed on top of the vial containing 0.2 mL of a given solvent (benzene, Et_2O, or toluene). Exposure of the crystal to the solvent vapor caused a color change from green to brown in less than 2 min. Visual inspection of the transformed crystal showed that it was no longer crystalline. Exposing this solid to ambient humidity brought back the initial green color over a few days.

Acknowledgment. The Natural Sciences and Engineering Research Council of Canada and Fonds Québécois de la Recherche sur la Nature et les Technologies are gratefully acknowledged for their financial support. The authors are grateful to Profs. C. Reber and G. Hanan for access to their Carry spectrometers and for valuable discussions.

IC070093M

(31) *SMART, Release 5.625, Bruker Molecular Analysis Research Tool*; Bruker AXS Inc.: Madison, WI, 2001.
(32) *SAINT, Release 7.06, Integration Software for Single Crystal Data*; Bruker AXS Inc.: Madison, WI, 2003.
(33) Sheldrick, G. M. *SHELXS, Program for the Solution of Crystal Structures*; University of Göttingen: Göttingen, Germany, 1997.
(34) (a) *SHELXTL, Release 5.10, The Complete Software Package for Single Crystal Structure Determination*; Bruker AXS Inc.: Madison, WI, 1997. (b) *SAINT, Release 7.06. Integration Software for Single Crystal Data*; Bruker AXS Inc.: Madison, WI, 2003. (c) *SMART, Release 5.625, Bruker Molecular Analysis Research Tool*; Bruker AXS Inc.: Madison, WI, 2001. (d) Sheldrick, G. M. *SADABS, Bruker Area Detector Absorption Corrections*; Bruker AXS Inc.: Madison, WI, 1996. (e) Sheldrick, G. M. *SHELXS97, Program for Crystal Structure Solution*; University of Göttingen: Göttingen, Germany, 1997. (f) Sheldrick, G. M. *SHELXL97, Program for Crystal Structure Refinement*; University of Göttingen: Göttingen, Germany, 1997. (g) Spek, A. L. *PLATON, Molecular Geometry Program*; University of Utrecht: Utrecht, Holland, 2000.
(35) Burnett, M. N.; Johnson, C. K. *ORTEPIII-Oak Ridge Thermal Ellipsoid Plot Program for Crystal Structure Illustrations, Technical Report ORNL-6895*; Oak Ridge National Laboratory: Oak Ridge, TN, 1996.